



Kinetic and isotherm study of Bromothymol Blue and Methylene blue removal using Au-NP loaded on activated carbon

M. Ghaedi^{a,*}, E. Nazari^b, R. Sahraie^c, M.K. Purkait^d

^aDepartment of Chemistry, Yasouj University, Yasouj, 75914-35, Iran

Tel./Fax: +98 741 2223048; email: m_ghaedi@mail.yu.ac.ir

^bDepartment of Chemistry, Payame Noor University, 19395-9697 Tehran, Iran

^cDepartment of Chemistry, Ilam University, Ilam, Iran

^dDepartment of Chemical Engineering, Indian Institute of Technology Guwahati, Guwahati 781039, Assam, India

Received 6 March 2012; Accepted 6 May 2013

ABSTRACT

In this research, the efficiency of gold nanoparticle loaded on activated carbon (Au-NP-AC) was used for the removal of Methylene blue (MB) and Bromothymol Blue (BTB) from aqueous solutions. The effect of various parameters such as solution pH, initial dye concentration, amount of Au-NP-AC, and temperature on the extent of dye adsorption was investigated. The performances of two dye adsorption capacities were compared. The adsorption equilibrium data were analyzed using Langmuir, Freundlich, Temkin, Dubinin–Radushkevich, and Harkins–Jura isotherm models. It was seen that Langmuir models represented the equilibrium data well with adsorption capacity of 40.65 and 95.24 mg g⁻¹ for MB and BTB, respectively. Kinetic data revealed that the adsorption of both the dyes on the adsorbent surface followed pseudo-second-order model.

Keywords: Adsorption; Methylene blue (MB); Bromothymol blue (BTB); Kinetic; Thermodynamic

1. Introduction

Various dyes are widely used in many industries such as textile, paper, and plastics to color their products. Their entrance and mixing with huge amounts of industrial waste to water lead to generation of highly colored effluent. Dyes are fast and easily detectable contaminants in water causing blocking of sunlight penetration (essential for many photo-initiated chemicals) and reactions leading to a decrease in the oxygen level and changes in the aquatic life. Synthetic dyes have high solubility in water and are frequently found

in trace quantities in industrial wastewater. Water contamination becomes a serious issue and generally produced dyes are discharged directly into aqueous effluents [1–4]. Most of the dyes are stable in the presence of light, heat and oxidizing agents, biodegradation, and also resistant to aerobic digestion [5–7]. Therefore, treatment of dyes is a serious rigid problem and is difficult to treat via conventional biological, chemical, and photochemical processes [8–10]. Most of these methods suffer from limitations such as expensive procedure and generation of huge amount of toxic waste, which make them non-efficient processes [11]. The adsorption based on application of various

*Corresponding author.

metallic and semimetallic nanoparticles are designed to clean up aqueous contaminated water in short time [12–17].

Recently, nanoparticles have been widely used for dye adsorption due to unique properties of nanoparticles in terms of high amount of surface atom, high mechanical stability, thermal strength, electrical conductivity, thermal conductivity, and high surface area [18–20]. The size, surface structure, and interparticle interaction of nanomaterials determine their unique properties and improve their performances for application in many areas [21–34]. Among various categories of nanoscale materials, metallic nanoparticles have been widely applied for binding and removal of biological materials and organic compounds.

The objective of the present work is preparation and application of gold nanoparticle-loaded activated carbon (Au-NP-AC) for the removal of Methylene blue (MB) and Bromothymol Blue (BTB) following the optimization of various adsorption operating conditions. Experimental data are analyzed using various kinetic and equilibrium models. The performance of the prepared adsorbent was also evaluated and investigated at different experimental conditions.

2. Experimental

2.1. Instruments and reagents

All chemicals including NaOH, HCl, KCl, MB, and BTB with the highest purity available are purchased from Merck (Dermasdat, Germany). About 100 mg of MB and/or BTB was dissolved in 500 mL deionized water to prepare 200 mg L⁻¹ (stock solution) and the working solution was prepared by diluting these solutions. The determination of each dye concentration was carried out using Jusco UV-Visible spectrophotometer model V-570 at a wavelength of 431 and 610 nm for MB and BTB, respectively. The pH/Ion meter model-686 and thermometer Metrohm was used for the adjustment of pH and temperature, respectively. Activated carbon (AC) (gas chromatographic grade, 60–80 mesh from Merck) was soaked in hydrochloric acid for two days and then washed with water and dried at 110°C for one day. After filtering, the content was washed with distilled deionized water and dried at 95°C for 5 h. Au-NPs-AC was synthesized and characterized according to our previous work reported elsewhere [35].

2.2. Batch adsorption experiments

The influence of variables including pH, amount of adsorbent, contact time, and initial dye concentra-

tion on the adsorptive removal of MB and BTB were investigated in batch mode. In each experiment, 50 mL of dyes in a 100 ml erlenmeyer flask was agitated and stirred at 350 rpm at constant temperature. The obtained experimental data at various times, temperature, and concentration was fitted to different models to evaluate and calculate the kinetics, thermodynamic, and isotherm parameters for both dyes at desired pH. The solution pH was adjusted by the addition of dilute aqueous solutions of HCl and/or NaOH (1.0 M). The dye removal percentage was calculated using the following relationship:

$$\% \text{ dye removal} = ((C_o - C_t)/C_o) \times 100 \quad (1)$$

where C_o (mg L⁻¹) and C_t (mg L⁻¹) are the dye concentrations, initial and after time t , respectively. The equilibrium adsorption capacities of both the dyes were calculated according to following equation:

$$q_e = (C_o - C_e)V/W \quad (2)$$

where C_o (mg L⁻¹) and C_e (mg L⁻¹) are the initial and equilibrium dye concentrations in the solution, respectively. V is the volume of the solution (L), and W is the mass (g) of the adsorbent.

3. Results and discussion

3.1. Characterization of adsorbent

Efficient reduction of Au³⁺ ions via starch in alkaline solution lead to generation of Au-NP (colloidal solutions) that has unique absorption spectra in the UV-vis spectral region well known as surface plasmon resonance (SPR). It was observed that the SPR intensity increased at higher pH and shifted to lower wavelength from 540 to 525 nm that may be attributed to decrease in the size of Au-NP. The FESEM image of the Au nanoparticles in (Fig. 1) shows the semispherical shape and uniform size (20–60 nm), which was also confirmed by the TEM analysis (Fig. 2 (a)). The exact crystalline structure of Au nanoparticles was determined by electron diffraction (ED) analysis and shown in Fig. 2(b). From the figure, it may be concluded that the prepared Au-NPs are cubic nanocrystalline in nature [20].

3.2. Characteristic of adsorbates

Bromothymol blue (also known as bromothymol sulfone phthalein) is a chemical indicator (Fig. 3) for weak acids and bases. The BTB was also used for observing photosynthetic activities and as respiratory

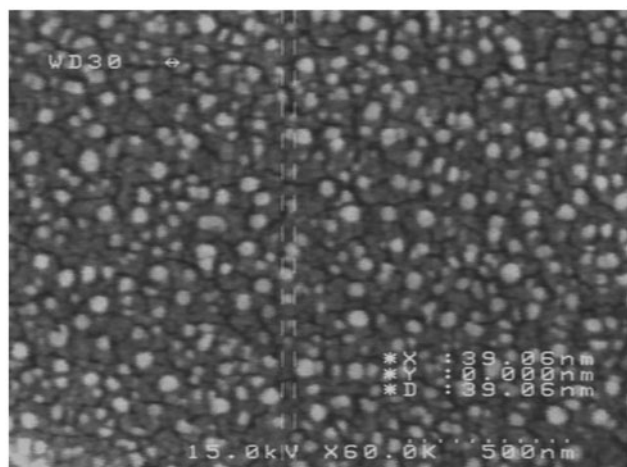


Fig. 1. FESEM image of the Au-NP loaded on activated carbon.

indicators. In acidic, alkaline, and neutral media, this dye shows yellow, blue, and bluish green color, respectively. MB is a heterocyclic aromatic compound (molecular formula of $C_{16}H_{18}N_3SCl$) that has many applications in different fields such as biology and chemistry. At room temperature, it appears as a solid, odorless, dark green powder which yields a blue aqueous solution. MB should not be confused with methyl blue (another histology stain) or with the methyl violets often used as pH indicators.

3.3. Effect of pH

Solution pH affects both aqueous chemistry and surface binding sites of the adsorbents. At higher pH, both the adsorbent surface and MB or BTB surface are neutral. The effect of initial pH on dye removal in the pH range of 2–8 at room temperature and 25 mg L^{-1} of MB and BTB onto 0.02 g of Au-NP-AC was investigated. The pH-dependent adsorption performances

are shown in Figs. 4(a) and (b) for BTB and MB, respectively. It may be seen that the maximum uptake of the BTB and MB is obtained at pH of 6 and 7, respectively using Au-NP-AC. At lower pH, the various functional groups of activated carbon protonated and due to electrostatic repulsion between dye molecules and positive surface of adsorbent, the removal percentage significantly decreased. The increase in removal percentage was due to interaction comprising of hydrogen bonding, π - π , and soft-soft interaction through nitrogen–Au atom.

3.4. Effect of adsorbent dosage

The amount of adsorbent and its surface area has a significant influence on the amount of dye adsorption. The effective surface area was increased with the addition of amount of NP and hence the extent of adsorption was also increased. In the proposed adsorbent, both Au atoms and different functional groups of AC such as hydroxyl, carboxylic, and carbonyl group act as reactive sites. It may be seen from Fig. 5 that by increasing the amount of adsorbent till 0.02 g for both dyes, the removal percentage increased rapidly due to the increase in the surface area and reactive sites of adsorbent, while further addition has no significant effect on the dye adsorption. This was due to the fact that most of the available sites had already been occupied by the adsorbed dye molecules. Therefore, 0.02 g of Au-NP-AC has been selected for subsequent work.

3.5. Effect of initial dye concentration on adsorption of MB and BTB

The influence of BTB and MB initial concentration in the range of 10 – 40 mg L^{-1} on their removal percentages and the actual amount of adsorbed dyes was investigated and results are shown in Figs. 6(a) and (b),

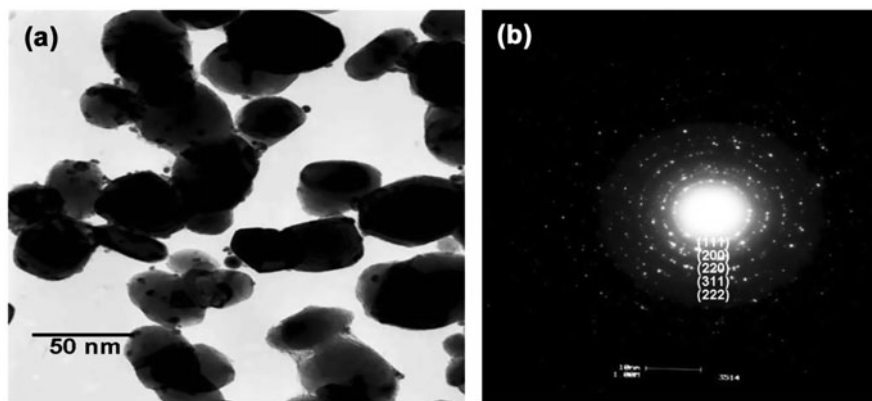


Fig. 2. (a) Typical TEM image of the starch-stabilized Au nanoparticles and (b) ED pattern of the Au nanoparticles.

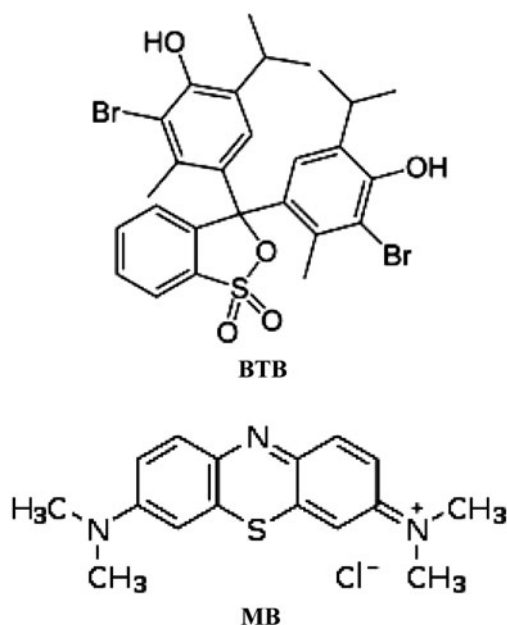


Fig. 3. Structure of dye molecules.

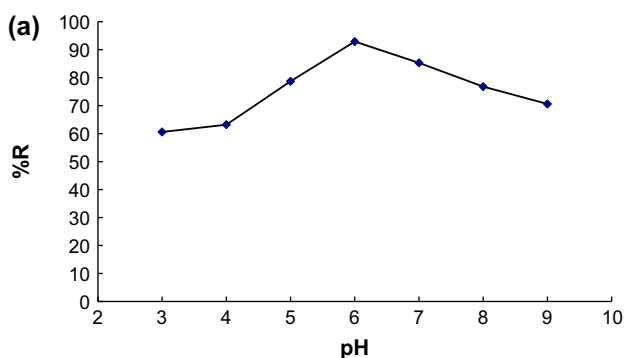


Fig. 4(a). Effect of pH on the removal of BTB by Au-NP-AC at room temperature, contact time: 15 min, adsorbent dosage: 0.4 g L^{-1} , and dye concentration: 10 mg L^{-1} .

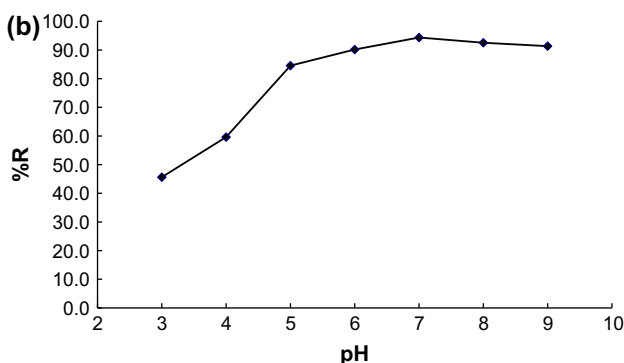


Fig. 4(b). Effect of pH on the removal of MB by Au-NP-AC at room temperature, contact time: 15 min, adsorbent dosage: 0.4 g L^{-1} , and dye concentration: 10 mg L^{-1} .

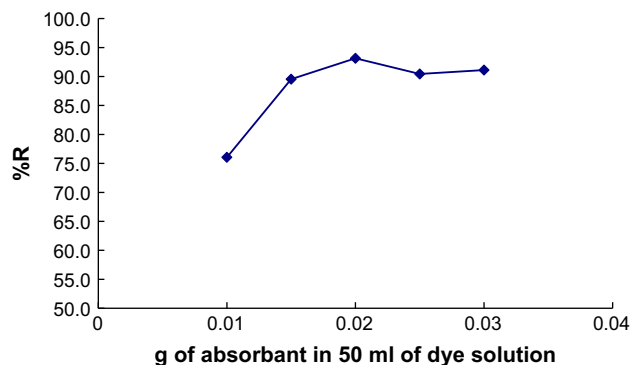


Fig. 5. Effect of Au-NP-AC dosage on MB removal from 50 mL of 10 mg L^{-1} of dye solution at pH 7 and room temperature.

respectively. It was observed (figure not shown) from the figure that the maximum amount of dye adsorption took place within the contact time of 20 min and attained equilibrium thereafter. This indicates that the rate of adsorption is very fast. Data have been taken up to 35 min of operation, which is more than sufficient to attain equilibrium. After that, no significant change in the extent of adsorption was observed. From the figures, it is evident that for lower initial concentration of dye, the adsorption is very fast. The percent removal of dye decreases with the increase in initial concentration of both dyes because of the fact that with the increase in dye concentration, there will be increased competition for the active adsorption sites and the adsorption process will increasingly slow down.

3.6. Effect of contact time on dyes adsorption

The results of adsorption with increasing contact time are presented in Fig. 7. The increase in contact time at 400 rpm stirring rate leads to enhancement in the dye adsorption. The adsorption is a fast process, so about 95% of the ultimate dye removal took place within the first 20 min that may be attributed to the high affinity and interaction between adsorbent and dyes. Subsequently, the amounts of adsorption reached a limiting value beyond which no significant improvement in adsorption took place. Final equilibrium adsorptions for both the dyes occurred at about 30 min; this time was considered as the equilibrium time in kinetic adsorption experiments.

3.7. Adsorption isotherms and kinetics

3.7.1. Kinetic modeling

An ideal adsorbent for the treatment of wastewater must not only have a large adsorption capacity but it has to have fast adsorption rate as well. The efficiency

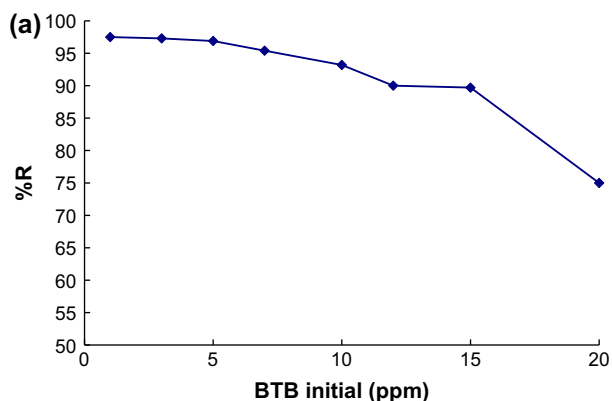


Fig. 6(a). Effect of initial dye concentration on removal of BTB at 0.4 g L^{-1} of Au-NP-AC at pH 6 and room temperature.

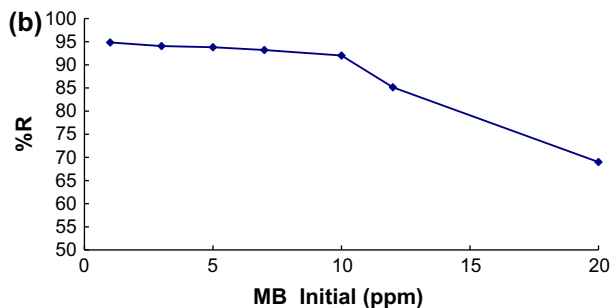


Fig. 6(b). Effect of initial dye concentration on removal of MB at 0.4 g L^{-1} of Au-NP-AC at pH 7 and room temperature.

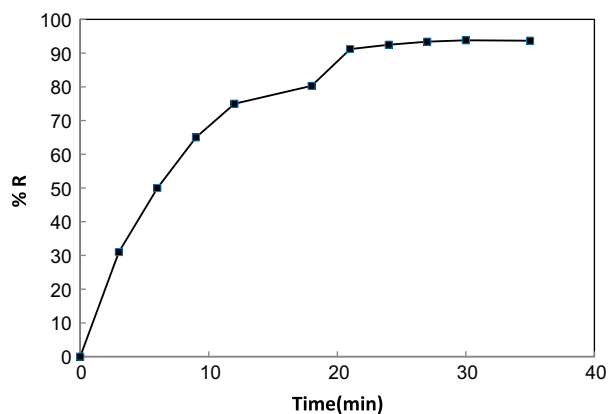


Fig. 7. Effect of contact time on MB adsorption.

and adsorption rates are good criteria for the selection of adsorbent. Conventional kinetic models including (1) pseudo-first-order kinetic model [36]; (2) pseudo-second-order kinetic model [37]; (3) and intraparticle diffusion model [38] were applied in this research for fitting the experimental data to evaluate the respective

parameters of each model and obtain some information about the adsorption mechanism such as adsorbent surface, chemical reaction, and/or diffusion mechanisms. The parameters of the kinetic models can be obtained by suitable linearization procedures followed by both linear and/or nonlinear regression analysis [39,40]. Two diffusion mechanisms are involved in the adsorption rate: pore diffusion (diffusion within the pore volume) and surface diffusion (diffusion along the surface of the pores). Pore diffusion has lower importance with respect to surface diffusion for nanoparticles adsorbent [41,42].

3.7.2. Pseudo-first-order equation

Generally, by plotting $\log(q_e - q_t)$ vs. t (linear relationship), k_1 and q_e can be evaluated from the slope and intercept of the respective line. The difference between the intercept and q_e means that the reaction is not likely to be first-order reaction, while it may have high correlation coefficients. It was found that the model is applicable for explanation of experimental data at initial stages but cannot be applied for the entire adsorption process. This indicates that the adsorption of MB and BTB is not a first-order reaction [43]. Furthermore, the calculated (q_e) value significantly differs from experimental q_e values (Table 1). This shows that the adsorptions of MB and BTB onto Au-NP-AC do not follow the first-order reaction.

3.7.3. Pseudo-second-order equation

Values of k_2 and equilibrium adsorption capacity (q_e) were calculated from the intercept and slope of the plots of t/q_t vs. t , respectively. The values of R^2 and q_e also indicate that this equation leads to better results (Table 1). R^2 values for the pseudo-second-order kinetic model were found to be higher than 0.99 and the calculated q_e values are near to the experimental data which strongly support the idea of applicability of this model for real fitting experimental data concern to the MB and BTB adsorption onto Au-NP-AC.

3.8. Intraparticle diffusion model

Among the various adsorption pathways, the dyes' adsorption on active sites of adsorbents may occur via chemical reaction, ion-exchange, complexation and/or chelation mechanism such as hydrogen bonding, electron donor-acceptor and van der Waals interaction by the liquid phase through intraparticle mass transport rate [44]. The plot of q_t vs. $t^{0.5}$ for the initial dye

Table 1
Adsorption kinetic parameters of BTB and MB on 0.4 g L^{-1} of Au-NP-AC at pH 6 for BTB and 7 for MB at room temperature

Model	Condition	Parameter		Value	
		MB	BTB	MB	BTB
First-order kinetic: $\log(q_e - q_t) = \log(q_e) - k_1 t / 2.303$	Plot the values of $\log(q_e - q_t)$ vs. t to give a linear relationship from which k_1 and q_e can be determined from the slope and intercept, respectively.	k_1		0.14	0.05
		q_e (calc)		5.85	16.63
		R^2		0.98	0.96
Second-order kinetic: $t/q = 1/k_2 q_e^2 + 1/q_e t$	The slope and intercept of plot of t/q versus t , The correlation coefficients of all examined data were found very high ($R^2 \geq 0.99$) calculating the initial sorption rate, similar to the experimental data	$k_2 \times 10^{+3}$		44.3	23.2
		q_e (calc)		6.4	12.6
		R^2		0.99	0.99
Elovich: $q_t = 1/\beta \ln(\alpha\beta) + 1/\beta \ln(t)$	Plot of q_t vs. $\ln(t)$, Initial adsorption rate, de-sorption constant, Based on the adsorption capacity	h		3.69	3.82
		β		1.14	1.06
Intraparticle diffusion: $q_t = K_{diff} t^{1/2} + C$	Plot of q_t vs. $t^{0.5}$, three steps: film diffusion and intraparticle transport, The slowest of three steps controls the overall rate of the process, C gives an idea about the thickness of boundary layer	α		48.6	52.9
		R^2		0.96	0.94
		K_{diff}		0.37	0.27
q_e (exp) $q_e = (C_0 - C_e)V/W$	Discover the adsorption capacity of AC, dye concentrations of 50, 100, and 200 mg/L of ARS.	C		3.65	9.72
		R^2		0.92	0.87
		q_e (exp)		5.89	12.12

concentration of 25 mg L^{-1} shows its nonlinear nature and data points can be better represented by double linear section with a different slope (k_i) and intercept (C). The values of k and C along with their regression constant (R^2) for both dyes and their values are reported in Table 1. First straight lines (sharp slop for short time) indicate the transport of MB and BTB to the external surface of the adsorbent through film diffusion. Then, MB and BTB molecules entered into the solid phase particle (intraparticle diffusion) through pore diffusion in the second straight line.

3.8.1. Elovich model

The Elovich model [45] equation based on the adsorption capacity and the rate expression can be presented in a linear form as:

$$q_t = 1/\beta \ln(\alpha\beta) + 1/\beta \ln(t) \quad (3)$$

The plot of q_t vs. $\ln(t)$ should yield a linear relationship if the Elovich is applicable, while the slope and intercept are $(1/\beta)$ and $(1/\beta) \ln(\alpha\beta)$, respectively. The Elovich constants obtained from the slope and the intercept of the straight line are reported in Table 1.

3.9. Equilibrium isotherm models

Adsorption properties and equilibrium data (adsorption isotherms) describe how pollutants interact with adsorbent materials and are critical in optimizing the use of adsorbents [46,47]. The Langmuir model with a well-known assumption is represented in a linear form as:

$$C_e/q_e = 1/k_L Q_m + C_e/Q_m \quad (4)$$

where K_L is the Langmuir adsorption constant (L mg^{-1}) and Q_m is the theoretical maximum adsorption capacity (mg g^{-1}). The Langmuir (C_e/q_e vs. C_e) plot for adsorption of MB and BTB at room temperature was depicted and the value of Q_m and K_L constants and the correlation coefficients for Langmuir isotherm are presented in Table 2. The maximum monolayer capacity (Q_m) obtained from the Langmuir model was 40.6 mg g^{-1} for MB and 95.2 mg g^{-1} for BTB onto Au-NP-AC. The isotherms of MB and BTB on the adsorbent were found to be linear over the whole concentration range studied here. The correlation coefficients were extremely high ($R^2 > 0.99$), which confirm that due to the cationic nature of MB, electrostatic repulsion inhibits the formation of further adsorption layer.

The Freundlich model in linear form is shown below:

$$\log q_e = \log K_F + (1/n_F) \log C_e \quad (5)$$

where K_F ((mg/g)/(mg/l)^{1/n}) and n_F show the capacity and intensity of the adsorption. Table 2 shows the Freundlich adsorption isotherm constants and the respective correlation coefficients. $1/n_F$ and K_F constants are determined from the slope and intercept of the plot of $\log q_e$ against $\log C_e$. The value of $1/n_F$ (heterogeneity factor) is between 0 and 1. For heterogeneous surface, the $1/n_F$ value is close to 0 and the n_F value higher than unity shows favorable physical adsorption process.

The Temkin isotherm model [47] among adsorbate particles that lead to linear decrease in the heat of adsorption of all expression is given as:

$$q_e = RT/b \ln(K_T C_e) \quad (6)$$

Eq. (6) can be linearized as:

$$q_e = B_T \ln K_T + B_T \ln C_e \quad (7)$$

where $B_T = RT/b_T$, T is the absolute temperature in K, R the universal gas constant, $8.314 \text{ J mol}^{-1} \text{ K}^{-1}$, K_T is the equilibrium binding constant (L mg^{-1}), and B_T is related to the heat of adsorption. The constants obtained for the Temkin isotherm are shown in Table 2.

Dubinin–Radushkevich isotherm model can be represented as a linear equation (Table 2). The slope of the plot of $\ln q_e$ vs. ε^2 gives K ($\text{mol}^2/\text{kJ}^{-2}$) and the intercept shows the adsorption capacity (Q_m) (mg/g). The mean free energy of adsorption (E) can be calculated from the K value using the following relationship:

$$E = 1/(2K)^{1/2} \quad (8)$$

From various model parameters and the correlation coefficients shown in Table 2, it may be concluded that for adsorption of BTB and MB, Langmuir model was found to be best fitted mode.

Table 2
Various isotherm models and their calculated parameters

Isotherm equation	Parameters	MB	BTB
Langmuir: $C_e/q_e = (1/K_a Q_m) + C_e/Q_m$	Q_m (mg g^{-1}) K_a (L mg^{-1}) R^2 $X^2 = \sum [(q_{e,\text{exp}} - q_{e,\text{calc}})^2 / q_{e,\text{exp}}]$ from $i=1$ to $i=m$	40.65 0.12 0.99 0.002	95.24 0.38 0.99 3.46
Freundlich: $\ln q_e = \ln K_F + (1/n) \ln C_e$	$1/n$ K_F (L mg^{-1}) R^2 $X^2 = \sum [(q_{e,\text{exp}} - q_{e,\text{calc}})^2 / q_{e,\text{exp}}]$ from $i=1$ to $i=m$	0.53 5.84 0.98 0.20	0.37 27.96 0.92 8.40
Temkin: $q_e = B_1 \ln K_T + B_1 \ln C_e$	B_1 K_T (L mg^{-1}) R^2 $X^2 = \sum [(q_{e,\text{exp}} - q_{e,\text{calc}})^2 / q_{e,\text{exp}}]$ from $i=1$ to $i=m$	9.03 1.16 0.96 0.05	16.4 7.07 0.97 0.16
Dubinin and Radushkevich (D–R): $\ln q_e = \ln Q_m - K\varepsilon^2$, $\varepsilon = RT \ln(1 + 1/C_e)$	Q_m (mg g^{-1}) K ($\times 10^{+6}$) E (kJ/mol) = $1/(2K)^{1/2}$ R^2 $X^2 = \sum [(q_{e,\text{exp}} - q_{e,\text{calc}})^2 / q_{e,\text{exp}}]$ from $i=1$ to $i=m$	24.67 1.0 0.7 0.88 2.5	67.92 0.1 2.23 0.88 34.0
Harkins–Jura (H–J): $1/q_e^2 = (B_2/A) - (1/A) \log C_e$	A B_2 R^2 $X^2 = \sum [(q_{e,\text{exp}} - q_{e,\text{calc}})^2 / q_{e,\text{exp}}]$ from $i=1$ to m	75.7 1.31 0.81 2.9	526.3 1.15 0.57 43.4

4. Conclusion

The Au-NP-AC was synthesized, characterized, and applied for the removal of MB and BTB. It was observed that the efficiency of the adsorption process depends on parameters such as initial dye concentration, contact time, pH, dose of adsorbent, and type of dye. Analysis of experimental equilibrium data to the Langmuir, Freundlich and Temkin isotherms shows that the Langmuir is the best model for the interpretation of equilibrium data. The kinetic process and experimental time domain data of adsorption successfully fitted to the second-order kinetic models. The results demonstrate that the MB removal is a very fast process and the adsorption is a surface phenomenon. The surfaces are readily accessible to the dyes in the solution. A view glance to the result presented in this research shows that the Au-NP-AC exhibits lower adsorption capacity for MB (40.65 mg g^{-1}) compared to BTB (95.24 mg g^{-1}).

References

- [1] E. Rubin, P. Rodriguez, R. Herrero, J. Cremades, I. Barbara, M. Sastre de Vicente, Removal of Methylene Blue from aqueous solutions using as biosorbent *Sargassum muticum*: An invasive macroalga in Europe, *J. Chem. Technol. Biotechnol.* 80 (2005) 291–298.
- [2] T.A. Albanis, D.G. Hela, T.M. Sakellariades, T.G. Danis, Removal of dyes from aqueous solutions by adsorption on mixtures of fly ash and soil in batch and column techniques, *Int. J. Global Nest* 2 (2000) 237–244.
- [3] R.F.P.M. Moreira, M.G. Peruch, N.C. Kuhnen, Adsorption of textile dyes on alumina. Equilibrium studies and contact time effects, *Braz. J. Chem. Eng.* 15(1) (1998) 21–28.
- [4] A. Sari, M. Tuzen, Biosorption of cadmium(II) from aqueous solution by red algae (*Ceramium virgatum*): Equilibrium, kinetic and thermodynamic studies, *J. Hazard. Mater.* 157 (2008) 448–454.
- [5] R.A. Anayurt, A. Sari, M. Tuzen, Equilibrium, thermodynamic and kinetic studies of biosorption of Pb(II) and Cd(II) from aqueous solution by macrofungus (*Lactarius scrobiculatus*) biomass, *Chem. Eng. J.* 151 (2009) 255–261.
- [6] F. Taghizadeh, M. Ghaedi, K. Kamali, E. Sharifpour, R. Sahraei, M.K. Purkait, Comparison of nickel and/or zinc selenide nanoparticle loaded on activated carbon as efficient adsorbents for kinetic and equilibrium study of removal of Arsenazo (III) dye, *Powder Technol.* 245 (2013) 217–226.
- [7] M. Ghaedi, M. Ghayedi, S.N. Kokhdan, R. Sahraei, A. Daneshfar, Palladium, silver, and zinc oxide nanoparticles loaded on activated carbon as adsorbent for removal of bromophenol red from aqueous solution, *J. Ind. Eng. Chem.* 19 (2013) 1209–1217.
- [8] M. Ghaedi, F. Karimi, B. Barazesh, R. Sahraei, A. Daneshfar, Removal of reactive orange 12 from aqueous solutions by adsorption on tin sulfide nanoparticle loaded on activated carbon, *J. Ind. Eng. Chem.* 19 (2013) 756–763.
- [9] M. Ghaedi, B. Sadeghian, S.N. Kokhdan, A.A. Pebdani, R. Sahraei, A. Daneshfar, A. Mihandoost, Study of removal of Direct Yellow 12 by cadmium oxide nanowires loaded on activated carbon, *Mater. Sci. Eng. C* 33 (2013) 2258–2265.
- [10] M. Ghaedi, S.N. Kokhdan, Oxidized multiwalled carbon nanotubes for the removal of methyl red (MR): Kinetics and equilibrium study, *Desalin. Water Treat.* 49 (2012) 317–325.
- [11] M. Ghaedi, S. Heidarpour, S. Nasiri Kokhdan, R. Sahraei, A. Daneshfar, B. Brazesh, Comparison of silver and palladium nanoparticles loaded on activated carbon for efficient removal of Methylene blue: Kinetic and isotherm study of removal process, *Powder Technol.* 228 (2012) 18–25.
- [12] M. Ghaedi, Comparison of cadmium hydroxide nanowires and silver nanoparticles loaded on activated carbon as new adsorbents for efficient removal of Sunset yellow: Kinetics and equilibrium study, *Spectrochim. Acta Part A* 94 (2012) 346–351.
- [13] M. Ghaedi, P. Ghobadzadeh, S. Nasiri Kokhdan, M. Soylyak, Oxidized multiwalled carbon nanotubes as adsorbents for kinetic and equilibrium study of removal of 5-(4-dimethyl amino benzylidene)rhodanine, *Arabian J. Sci. Eng.* 38 (2013) 1691–1699.
- [14] M. Ghaedi, B. Sadeghian, A.A. Pebdani, R. Sahraei, A. Daneshfar, C. Duran, Kinetics, thermodynamics and equilibrium evaluation of direct yellow 12 removal by adsorption onto silver nanoparticles loaded activated carbon, *Chem. Eng. J.* 187 (2012) 133–141.
- [15] M. Ghaedi, J. Tashkhourian, A.A. Pebdani, B. Sadeghian, F.N. Ana, Equilibrium, kinetic and thermodynamic study of removal of reactive orange 12 on platinum nanoparticle loaded on activated carbon as novel adsorbent, *Korean J. Chem. Eng.* 28 (2011) 2255–2261.
- [16] W.T. Tsai, C.Y. Chang, M.C. Lin, S.F. Chien, H.F. Sun, M.F. Hsieh, Adsorption of acid dye onto activated carbons prepared from agricultural waste bagasse by ZnCl_2 activation, *Chemosphere* 45 (2001) 51–58.
- [17] M. Ghaedi, A. Ansari, M.H. Habibi, A.R. Asghari, Removal of malachite green from aqueous solution by zinc oxide nanoparticle loaded on activated carbon: Kinetics and isotherm study original research article, *J. Ind. Eng. Chem.* (in press). Available online 30 April 2013.
- [18] G.C. Gerald, S.D. Russel, *J. Am. Chem. Soc.* 113 (1991) 1636–1639.
- [19] M.J. Iqbal, M.N. Ashiq, Adsorption of dyes from aqueous solutions on activated charcoal, *J. Hazard. Mater. B* 139 (2007) 57–66.
- [20] Z. Wu, H. Joo, I.-S. Ahn, S. Haam, J.-H. Kim, K. Lee, Organic dye adsorption on mesoporous hybrid gels, *Chem. Eng. J.* 102 (2004) 277–282.
- [21] X. Li, L. Zheng, L. Huang, O. Zheng, Z. Lin, L. Guo, B. Qiu, G. Chen, Adsorption removal of crystal violet from aqueous solution using a metal-organic frameworks material, copper coordination polymer with dithiooxamide, *J. Appl. Polym. Sci.* 129(5) (2013) 2857–2864.
- [22] M. Alkan, O. Demirbas, S. Celikcapa, M. Dogan, Sorption of acid red 57 from aqueous solution onto sepiolite, *J. Hazard. Mater.* 116 (2004) 135–145.
- [23] K. Ravikumar, B. Deebika, K. Balu, Decolourization of aqueous dye solutions by a novel adsorbent: Application of statistical designs and surface plots for the optimization and regression analysis, *J. Hazard. Mater.* 122 (2005) 75–83.
- [24] B. Guo, L. Hong, H.X. Jiang, Macroporous poly(calcium acrylatedivinyle/benzene) bead—A selective orthophosphate sorbent, *Ind. Eng. Chem. Res.* 42 (2003) 5559–5567.
- [25] F.A. Pavan, Y. Gushikem, A.S. Mazzocato, S.L.P. Dias, E.C. Lima, Statistical design of experiments as a tool for optimizing the batch conditions to methylene blue biosorption on yellow passion fruit and mandarin peels, *Dyes Pigm.* 72 (2007) 256–266.
- [26] F.A. Pavan, E.C. Lima, S.L.P. Dias, A.C. Mazzocato, Methylene blue biosorption from aqueous solutions by yellow passion fruit waste, *J. Hazard. Mater.* 150 (2008) 703–712.
- [27] E.C. Lima, B. Royer, J.C.P. Vaggetti, N.M. Simon, B.M. da Cunha, F.A. Pavan, E.V. Benvenuti, R.C. Veses, C. Airoidi, Application of Brazilian pine-fruit shell as a biosorbent to removal of reactive red 194 textile dye from aqueous solution: Kinetics and equilibrium study, *J. Hazard. Mater.* 155 (2008) 536–550.

- [28] J.C.P. Vagheti, E.C. Lima, B. Royer, J.L. Brasil, B.M. da Cunha, N.M. Simon, N.F. Cardoso, C.P.Z. Norena, Application of Brazilian-pine fruit coat as a biosorbent to removal of Cr(VI) from aqueous solution-Kinetics and equilibrium study, *Biochem. Eng. J.* 42 (2008) 67–76.
- [29] S. Lagergren, Zur theorie der sogenannten adsorption gelöster stoffe, *K. Svenska Vetenskapsakademiens. Handl.* 24 (1898) 1–39.
- [30] A.A. Ahmed, B.H. Hameed, N. Aziz, Adsorption of direct dye on palm ash: Kinetic and equilibrium modeling, *J. Hazard. Mater.* 141 (2007) 70–76.
- [31] M. Ghaedi, A. Shokrollahi, H. Tavallali, F. Shojaeipoor, B. Keshavarzi, H. Hossainian, M. Soylak, M.K. Purkait, Activated carbon and multiwalled carbon nanotubes an efficient adsorbents for kinetic and equilibrium study of removal of Arsenazo (III) and methyl red dyes from waste water, *Toxicol. Environ. Chem.* 93 (2011) 438–449.
- [32] M. Soylak, Y.E. Unsal, M. Tuzen, Spectrophotometric determination of trace levels of Allura Red in water samples after separation and preconcentration, *Food Chem. Toxicol.* 49 (2011) 1183–1187.
- [33] M. Soylak, Y.E. Unsal, E. Yilmaz, M. Tuzen, Determination of Rhodamine B in soft drink, waste water and lipstick samples after solid phase extraction, *Food Chem. Toxicol.* 49 (2011) 1796–1799.
- [34] M. Ghaedi, H. Hossainian, M. Montazerzohori, A. Shokrollahi, F. Shojaeipoor, M. Soylak, M.K. Purkait, A Novel acorn based adsorbent for the removal of Brilliant Green, *Desalination* 281 (2011) 226–233.
- [35] G. Karimipour, M. Ghaedi, R. Sahraei, A. Daneshfar, M.N. Biyareh, Modification of gold nanoparticle loaded on activated carbon with bis(4-methoxysalicylaldehyde)-1,2-phenylenediamine as new sorbent for enrichment of some metal ions, *Biol. Trace Elem. Res.* 145 (2012) 109–117.
- [36] Y.S. Ho, G. McKay, Sorption of dye from aqueous solution by peat, *Chem. Eng. J.* 70 (1998) 115–124.
- [37] W.J. Weber, J.C. Morris, Kinetics of adsorption on carbon from solution, *J. Sanitary. Eng. Div. Am. Soc. Civil Eng.* 89 (1963) 31–59.
- [38] G. Crini, C. Robert, F. Gimbert, B. Martel, O. Adam, F. De Giorgi, The removal of Basic Blue 3 from aqueous solutions by chitosan-based adsorbent: Batch studies, *J. Hazard. Mater.* 153 (2007) 96–106.
- [39] G. McKay, H.S. Blair, J.R. Gardner, I.F. McConvey, Two-resistance mass transfer model for the adsorption of various dye-stuffs onto chitin, *J. Appl. Polym. Sci.* 30 (1985) 4325–4335.
- [40] G. Gibbs, J.M. Tobin, E. Guibal, Sorption of Acid Green 25 on chitosan: Influence of experimental parameters on uptake kinetics and sorption isotherms, *J. Appl. Polym. Sci.* 90 (2003) 1073–1080.
- [41] E. Guibal, P. McCarrick, J.M. Tobin, Comparison of the sorption of anionic dyes on activated carbon and chitosan derivatives from dilute solutions, *Sep. Sci. Technol.* 38 (2003) 3049–3073.
- [42] Y.S. Ho, G. McKay, D.A.J. Wase, C.F. Foster, Study on the sorption of divalent metal ions onto peat, *Adsorpt. Sci. Technol.* 18 (2000) 639–650.
- [43] J.J. Pignatello, F.J. Ferrandino, L.Q. Huangm, Elution of aged and freshly added herbicides from a soil, *Environ. Sci. Technol.* 27 (1993) 1563–1571.
- [44] M. Ghaedi, A. Shokrollahi, H. Hossainian, S. Nasiri Kokhdan, Comparison of activated carbon and multiwalled carbon nanotubes for efficient removal of Eriochrome cyanine R (ECR): Kinetic, isotherm, and thermodynamic study of the removal process, *J. Chem. Eng. Data.* 56 (2011) 3227–3235.
- [45] Y.H. Li, Z. Di, J. Ding, D. Wu, Z. Luan, Y. Zhu, Adsorption thermodynamic, kinetic and desorption studies of Pb^{2+} on carbon nanotubes, *Water Res.* 39 (2005) 605–609.
- [46] C. Lu, Y.-L. Chung, K.-F. Chang, Adsorption thermodynamic and kinetic studies of trihalomethanes on multiwalled carbon nanotubes, *J. Hazard. Mater.* B138 (2006) 304–310.
- [47] G. McKay, Use of adsorbents for the removal of pollutants from wastewater, CRC Press, Kowloon, 1995, p. 208.